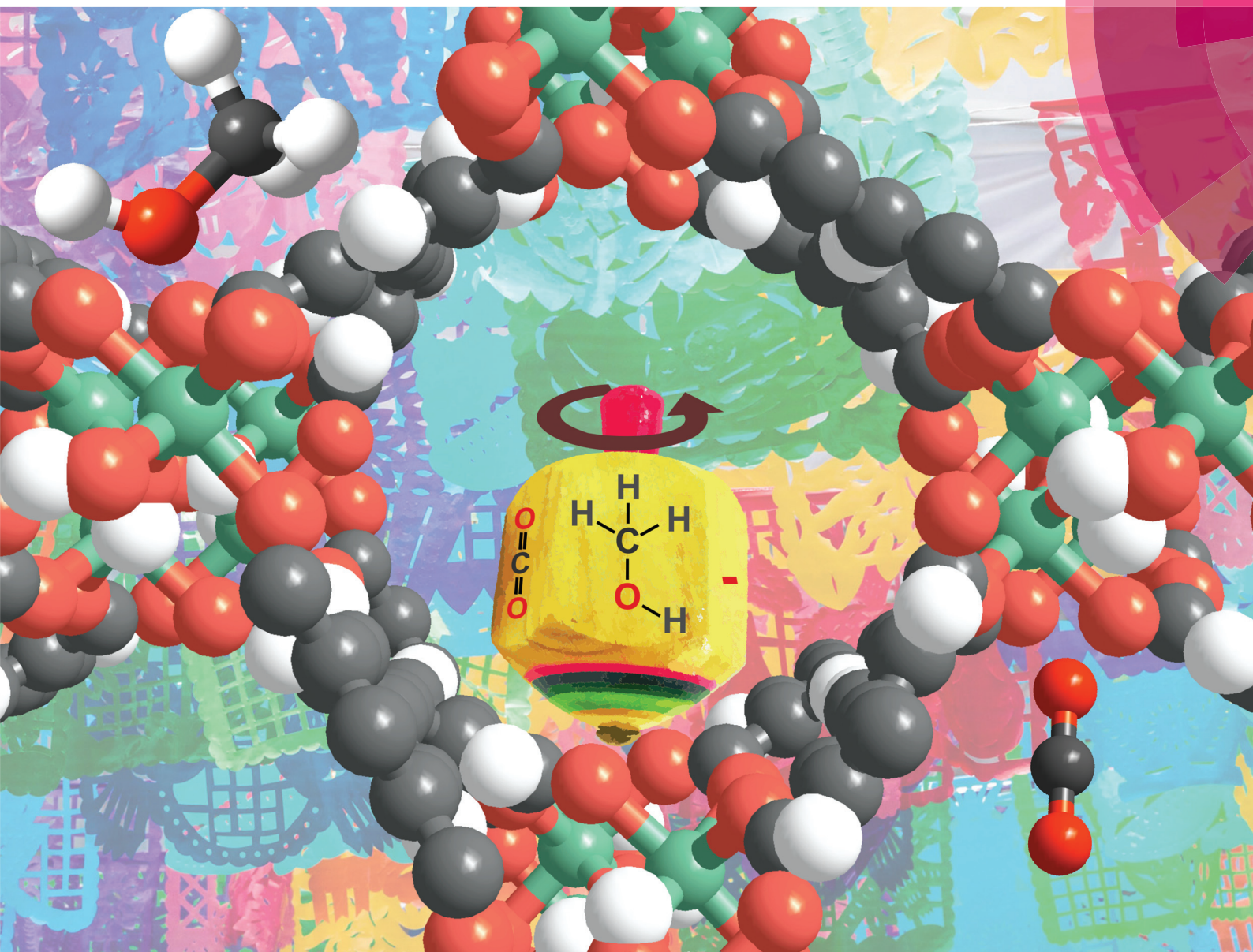


Dalton Transactions

An international journal of inorganic chemistry

rsc.li/dalton



ISSN 1477-9226



PAPER

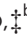



Guillaume Maurin, Ilich A. Ibarra *et al.*
Confined methanol within InOF-1: CO₂ capture enhancement

Cite this: *Dalton Trans.*, 2017, **46**, 15208Received 24th July 2017,
Accepted 14th August 2017

DOI: 10.1039/c7dt02709e

rsc.li/dalton

Confined methanol within InOF-1: CO₂ capture enhancement†

Elí Sánchez-González,  ‡^a Paulo G. M. Mileo,  ‡^b J. Raziel Álvarez,  ^a
Eduardo González-Zamora,  ^c Guillaume Maurin*^b and Ilich A. Ibarra  ^{*a}

The CO₂ capture performance of InOF-1 was optimised by confining small amounts of MeOH within its micropores (MeOH@InOF-1). In comparison with fully activated InOF-1, MeOH@InOF-1 shows a 1.30 and 4.88-fold increase in CO₂ capture capacity for kinetic and static isothermal CO₂ adsorption experiments respectively. Density functional theory calculations coupled with forcefield based-Monte Carlo simulations revealed that such an enhancement is assigned to an increase of the degree of confinement felt by the CO₂ molecules resulting from the formation of a lump at the vicinity of the μ₂-OH groups since MeOH strongly interacts with these adsorption sites and is thus highly localized in this region.

Introduction

Current studies have demonstrated how the confinement of different solvents, within porous materials, can significantly enhance the gas solubility in comparison with the values expected by using Henry's law, *i.e.* considering a linear evolution of the concentration of a dissolved gas with respect to its partial pressure above the solvent.¹ This phenomenon is well described in the literature as “gas-oversolubility”.² In fact, the oversolubility of different confined-solvents can dramatically modify the characteristic physicochemical properties such as the density, viscosity, specific heat and dielectric constant.³ A remarkable example was recently presented by Garcia-Garibay and co-workers⁴ who demonstrated a striking increase by 4 orders of magnitude of the dynamic viscosity of confined DMF within UCLA-R3. Luzar and Bratko⁵ predicted, by Monte Carlo calculations, the oversolubility of N₂ and O₂ up to a 10-fold increase when water molecules are confined in hydrophobic mesopores. Pera-Titus *et al.*^{1,6} demonstrated how the

confinement of CHCl₃, *n*-C₆H₁₄, H₂O, and EtOH in mesostructured materials considerably enhances H₂ solubility. By confining *N*-methyl-2-pyrrolidone, in the mesopores of MCM-41, Pellenq⁷ showed an outstanding 6-fold increment in CO₂ solubility. Farrusseng⁸ confined, within MIL-101(Cr), high amounts of *n*-hexane, *i.e.* 60% of the pore volume, affording an extraordinary 22-fold enhancement in H₂ uptake. In the context of CO₂ capture where solvents are confined in metal-organic frameworks (MOFs), the corner-stone investigation was presented by Chang and Llewellyn.⁹ When 40 wt% of H₂O is confined within the mesopores of MIL-100(Fe), a significant 5-fold increase of CO₂ uptake is achieved.⁹

It is worth emphasizing that gas oversolubility, as presented in the previous examples, was observed only in mesoporous materials. In fact, when referring to gas oversolubility it is required to incorporate *via* pre-adsorption or impregnation, high amounts of solvents before any gas uptake. On the other hand, when high quantities of solvents are confined within the micropores of MOF materials, it is not possible to enhance their CO₂ adsorption properties as demonstrated in UiO-66,⁹ InOF-1,¹⁰ NOTT-400¹¹ and NOTT-401¹² since gas oversolubility does not occur in microporous MOFs. However, when small amounts of solvents are confined within these microporous materials, an effective and efficient CO₂ capture enhancement was undoubtedly accomplished.¹³

Typically, Walton and co-workers¹⁴ showed CO₂ capture enhancements in microporous MOF materials by confining small amounts of H₂O. Recently, our research group showed the relevance of confining small amounts of pre-adsorbed H₂O within microporous MOFs in order to enhance their CO₂ capture properties.¹⁵ In addition to H₂O, we explored the confinement of other solvents within MOFs: DMF,¹⁶ EtOH,¹⁷ MeOH¹⁸ and *i*-PrOH.¹⁸ We evidenced the positive impact of all

^aLaboratorio de Físicoquímica y Reactividad de Superficies (LaFRoS), Instituto de Investigaciones en Materiales, Universidad Nacional Autónoma de México, Circuito Exterior s/n, CU, Del. Coyoacán, 04510 Ciudad de México, Mexico. E-mail: argel@unam.mx

^bInstitut Charles Gerhardt Montpellier, UMR-5253, Université de Montpellier, CNRS, ENSCM, Place E. Bataillon, 34095 Montpellier cedex 05, France. E-mail: guillaume.maurin@univ-montp2.fr; Fax: +52(55) 5622-4595

^cDepartamento de Química, Universidad Autónoma Metropolitana-Iztapalapa, San Rafael Atlixco 186, Col. Vicentina, Iztapalapa, C. P. 09340 Ciudad de México, Mexico

† Electronic supplementary information (ESI) available: TGA data, PXRD data, activation protocol, isosteric enthalpy of adsorption data and theoretical calculations. See DOI: 10.1039/c7dt02709e

‡ These authors contributed equally to this work.

these confined solvents on the CO₂ adsorption performances of a few microporous MOF materials.^{15–18} Particularly, for EtOH^{17a} and DMF,¹⁶ the interactions of these confined solvents with the InOF-1 MOF material that afforded a considerably enhanced CO₂ capture for this MOF were possible to visualise by single crystal X-ray diffraction.

Continuing with the progress of new CO₂ capture technologies,¹⁹ the uninterrupted development of hybrid MOF materials with high adsorption capacity, fast sorption kinetics and mild regeneration conditions,^{20,21} can contribute to the “the twelve principles of CO₂ chemistry” proposed by Poliakov.²² Here, we present the preparation of a hybrid solvent-loaded MOF material (MeOH@InOF-1) for CO₂ capture by confining small amounts of methanol (MeOH). In addition, the MeOH adsorption properties of InOF-1²³ are discussed along with the enhanced CO₂ adsorption properties of MeOH@InOF-1. Analysis of the preferential adsorption sites and the energetics in play for both MeOH and CO₂ as single components and a binary mixture is provided by a subtle combination of periodic Density Functional Theory (DFT) and force field-based Monte Carlo (MC) simulations. This computational work allows an understanding at the molecular level of the origin of the enhancement of the affinity of InOF-1 towards CO₂ in the presence of MeOH.

Experimental section

Synthetic preparations

InOF-1 was synthesised according to the procedure published previously by Hong and co-workers.²³ Thermogravimetric analysis (see Fig. S1, ESI†) and bulk powder X-ray diffraction patterns (see Fig. S2, ESI†) of the as-synthesised InOF-1 confirmed the structure of this microporous MOF material. Samples of the as-synthesised InOF-1 were acetone exchanged²⁴ and activated at 453 K for two hours (either under 10^{−3} bar, static experiments, or with a constant flow of N₂ gas, dynamic experiments). N₂ adsorption isotherms for activated InOF-1, at 77 K, were performed to estimate a BET area (0.01 < P/P₀ < 0.04) of 1065 m² g^{−1} and a pore volume of 0.37 cm³ g^{−1}.

Sorption isotherms for N₂, CO₂ and MeOH

N₂ sorption isotherms (up to 1 bar and 77 K) were performed on a Belsorp mini II analyser under vacuum (10^{−3} bar). CO₂ adsorption–desorption isotherms, up to 1 bar and 196 K, were carried out on a Belsorp HP (High Pressure) analyser. MeOH isotherms were recorded in a DVS Advantage 1 instrument from Surface Measurement Systems. Ultra-pure grade (99.9995%) N₂ and CO₂ gases were purchased from PRAXAIR.

Kinetic CO₂ uptake experiments

Kinetic CO₂ capture experiments were carried out on a thermobalance (Q500 HR, from TA) at 303 K with a constant CO₂ flow of 60 mL min^{−1}.

Computational details

Periodic Density Functional Theory (DFT) calculations were first performed to optimize the geometry of the empty InOF-1, CO₂@InOF-1 and MeOH@InOF-1 structures starting with the crystal structure of InOF-1 previously published²³ and using the PBE functional²⁵ combined with the DNP basis set²⁶ as implemented in Dmol3. We considered for both CO₂ and MeOH the loading explored experimentally, *i.e.* 5.3 wt% and 2 wt% respectively.

Monte Carlo simulations in the NVT ensemble were carried out at 303 K to predict the adsorption behavior of CO₂ and MeOH as single components and a mixture in InOF-1. The same loadings than in the DFT calculations were considered for both molecules, and the simulation box was made of 8 (2 × 2 × 2) unit cells of the MOF. The host/guest and guest/guest interactions were treated using Lennard–Jones (LJ) potential and coulombic contributions. All-atom charged models were selected for both CO₂²⁷ and MeOH²⁸ while the atoms of the MOF framework were described by LJ charged sites with parameters extracted from the generic force field UFF²⁹ (inorganic node) and Dreiding³⁰ (organic node). The corresponding LJ parameters and partial charges are described in the ESI (Table S1 and Fig. S1†).

Results and discussion

Methanol sorption studies

Methanol (MeOH) adsorption–desorption analyses were studied for InOF-1. A sample of the acetone-exchanged InOF-1 was positioned in an analyser cell (DVS Advantage 1 instrument) and activated (see Synthetic preparations, static experiments). After the activated InOF-1 sample was cooled down to 303 K, a methanol adsorption–desorption isotherm was performed from %P/P₀ = 0 to 90 (Fig. 1), where P₀ is the saturated vapour pressure of methanol at the working temperature (12.88 and 21.76 kPa at 293 and 303 K respectively).

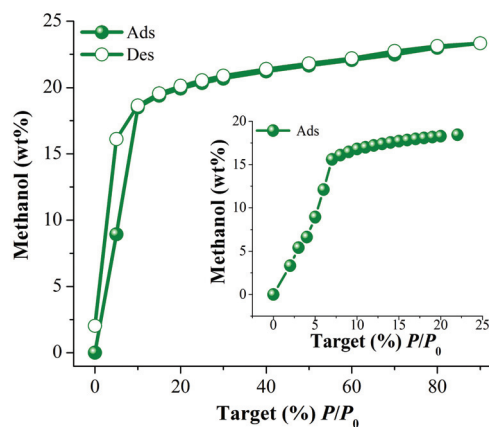


Fig. 1 Methanol (MeOH) adsorption isotherm at 303 K of InOF-1 from %P/P₀ = 0 to 90. Solid circles represent adsorption, and open circles show desorption. The inset shows the MeOH adsorption isotherm at 303 K from %P/P₀ = 0 to 22.

In Fig. 1 it is possible to observe a rapid MeOH uptake from the beginning of the experiment up to approximately $\%P/P_0 = 10$ (18.49 MeOH wt%). Above this pressure, we observe a quasi-plateau associated with a very slow uptake increase up to $\%P/P_0 = 85$ with a total MeOH adsorbed amount of ~ 23.3 wt%. The steep increase of the adsorption uptake at low pressure clearly indicates that InOF-1 shows a high affinity towards MeOH.

This was further confirmed by the evaluation of the isosteric heat of adsorption ($\Delta H = -41$ kJ mol⁻¹, at low MeOH coverage) that was obtained from the consideration of adsorption isotherms calculated at two different temperatures and the application of the Clausius–Clapeyron equation (303 and 293 K see Fig. S3 and S4 ESI†).

Usually for MOF materials, the use of the Clausius–Clapeyron and Virial equations is very well known and we, previously, successfully used these mathematical approaches.³¹ This calculation is also fully consistent with the MC-simulated adsorption enthalpy for MeOH (-40.8 kJ mol⁻¹), both values being slightly higher than the molar enthalpy of vaporisation for MeOH³² (-38.28 kJ mol⁻¹). Finally, the ΔH for MeOH is in good agreement with the value already reported for MOFs that show bridging μ_2 -OH functional groups.³³

The lack of an inflexion point in the shape of the isotherms (Fig. 1 and 2), suggests only one domain of adsorption.¹¹ The overall MeOH isotherm-shape shows a characteristic type-I isotherm (IUPAC) and a minor hysteresis loop (at 303 K and $\%P/P_0 = 0$ –10) was observed with marked stepped profiles in the desorption branch (Fig. 1, open circles). The pore diameter of InOF-1 (~ 7.5 Å)²³ is considerably larger than the kinetic diameter of MeOH (3.6 Å). Thus, this hysteresis cannot be correlated with the arguments of “kinetic trapping”, as suggested by many research groups for other materials (see ref. 34 for some representative examples). Instead, the observed hysteresis might be due to the relatively strong host–guest interactions mentioned above.

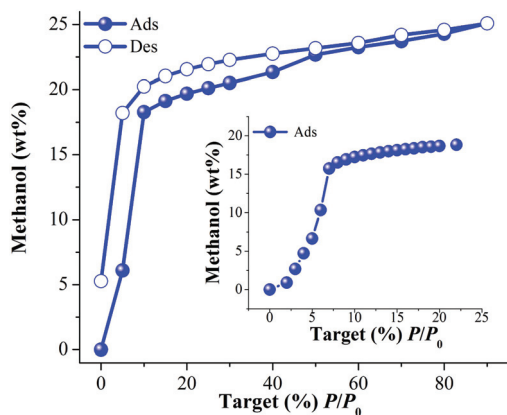


Fig. 2 Methanol (MeOH) adsorption isotherm at 293 K of InOF-1 from $\%P/P_0 = 0$ to 90. Solid circles represent adsorption, and open circles show desorption. The inset shows the MeOH adsorption isotherm at 293 K from $\%P/P_0 = 0$ to 22.

The MeOH isotherm at 293 K was similar to the sorption experiment at 303 K with two main differences: the total uptake at $\%P/P_0 = 90$ (~ 25.1 MeOH wt%) is slightly higher (~ 23.3 wt%) and the hysteresis is much more pronounced. These results are consistent with the lower operational temperature (293 K); when reducing the temperature of the experiment, a more efficient packing of the molecules can be favored by a more localized interaction between MeOH and the μ_2 -OH functional groups. Thus, a slightly higher total uptake and more pronounced hysteresis are expected as previously observed for EtOH at 293 K in InOF-1.^{17a}

The DFT-optimized structure of MeOH@InOF-1 (Fig. 3a) evidences a preferential sitting of the guest molecules at the vicinity of the μ_2 -OH groups that leads to the formation of a hydrogen bond between O(MeOH) and H(μ_2 -OH) associated with a characteristic distance of 1.90 Å (Fig. 3a), similarly to what was previously reported for ethanol (EtOH)^{17a} in the same MOF. The same adsorption behavior was also observed in our MC simulations (Fig. 2b). The center of mass distribution averaged over all the configurations generated by MC simulations for a low CH₃OH loading (2 wt%) reveals that the arrangement of the guest is highly localized near the μ_2 -OH groups (Fig. 3b) consistent with a strong host/guest interaction as suggested by the relatively high calculated and experimental adsorption enthalpy.

CO₂ capture studies

Dynamic and isothermal kinetic CO₂ capture experiments were carried on the acetone-exchanged samples of InOF-1. These samples were activated (see Synthetic preparations, static

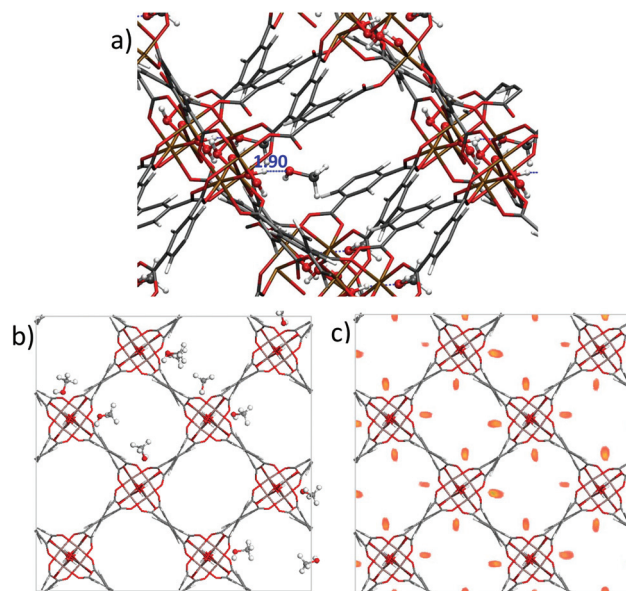


Fig. 3 DFT-optimized structure for MeOH@InOF-1 showing the preferential adsorption of the guest towards the μ_2 -OH groups. (a) Illustration of the preferential adsorption sites evidenced by MC simulations (b) and the map of the center of mass distribution of MeOH averaged over all the configurations generated by MC simulations.

experiments) on a thermobalance Q500 HR. After the activated sample was cooled down to 303 K (under a N₂ flow), the N₂ purge flow was switched to 60 mL min⁻¹ of CO₂. Fig. 4 shows the kinetic CO₂ uptake experiment at 303 K for activated InOF-1. The maximum weight percentage gain corresponds to the maximum amount of CO₂ captured. This amount of 5.2 wt% was quickly reached after only 5 min and it was constant until the end of the experiment (10 min), Fig. 4 (InOF-1).

The DFT-optimized structure of CO₂@InOF-1 (Fig. S6†) evidences that similarly to MeOH, CO₂ preferentially adsorbs at the vicinity of the μ₂-OH groups however with an interacting distance which is much longer (2.95 Å). This is consistent with a much lower adsorption enthalpy calculated by MC (-21 kJ mol⁻¹) for this guest as compared to MeOH (-40.8 kJ mol⁻¹) and a much more scattered distribution of the center of mass of the CO₂ in the pores of the MOF framework (Fig. S3†).

An acetone-exchanged sample of InOF-1 was activated (*vide supra*), cooled down to 303 K (under N₂) and fully saturated with MeOH (see the ESI†). By following an activation protocol (see the ESI†) the residual amount of confined MeOH was equal to 2 wt%. In order to corroborate the reproducibility of the activation protocol for InOF-1, we carried out 5 independent experiments (see the ESI†) which provided us, approximately, the same residual amount of MeOH. Hereinafter, this sample will be referred to as MeOH@InOF-1.

We decided to work only with small amounts of confined MeOH, within InOF-1, motivated by our previous experimental work on EtOH (2.6 wt%) confined in the micropores of InOF-1,^{17a} which led to the formation of hydrogen bonds with the μ₂-OH groups and to a significant improvement of the overall CO₂ capture (2.7 fold increase).^{17a}

The effect of the μ₂-OH groups present in different MOFs on the strength of interactions with solvent molecules is also well documented from a computational standpoint.^{35–37}

A kinetic CO₂ adsorption experiment (303 K) was performed on a MeOH@InOF-1 sample. The total amount of CO₂ adsorbed was equal to 6.9 wt%. This CO₂ uptake was achieved at ~4 min and remained constant until the last part of the

experiment (10 min) (Fig. 4, MeOH@InOF-1). The samples of MeOH@InOF-1 were synthesised with anhydrous methanol (<0.005% water) and methanol (reagent alcohol, 95%). The kinetic CO₂ capture experiments exhibit no difference. Other residual amounts of MeOH (3%, 4% and 5%) were tested and the best result was obtained with 2 wt% of confined MeOH. Thus, the dynamic CO₂ capture, at 303 K, was approximately 1.3-fold improved (from 5.2 wt% to 6.9 wt%), after confining small amounts of MeOH within InOF-1. Since ethanol is a bigger molecule than methanol, it provides a stronger confinement effect which enhances the CO₂ capture even more.

Continuing with the investigation of the CO₂ adsorption properties of MeOH@InOF-1, static and isothermal CO₂ adsorption experiments (increasing the partial pressure from 0 to 1 bar at 196 K) were carried out. The adsorption of CO₂ at 303 K is rather complicated since it is very close to the critical temperature of CO₂.³³ At 303 K the density (δ_{CO₂}) of CO₂ adsorbed is difficult to estimate because the CO₂ saturation pressure is really high and therefore the range of P/P₀ is limited to only 0.02 at sub-atmospheric pressures.³⁸ Additionally, it has been postulated that adsorption in well-defined micropores occurs by a pore-filling mechanism rather than surface coverage.^{38,39} For example, N₂ molecules (77 K) can fill micropores in a liquid-like fashion at very low relative pressures under 0.01. Conversely, CO₂ adsorbed at ambient temperatures can only form a monolayer on the walls of microporous materials.³⁹ Thus, in order to achieve pore-filling micropores and a much better and precise description of the CO₂ adsorption properties of these MOFs, CO₂ gas adsorption experiments at 196 K are highly desired.⁴⁰

For this purpose, a CO₂ static sorption-experiment at 196 K was performed on an activated (see Synthetic preparations, static experiments) sample of InOF-1 with a total CO₂ uptake of 24.2 wt%, (Fig. 5, InOF-1). Then, a MeOH@InOF-1 sample was quickly mounted in a high-pressure cell (Belsorp HP) and carefully evacuated to eliminate any absorbed moisture. The CO₂ adsorption-desorption experiment from 0 to 1 bar and 196 K showed a CO₂ uptake at low pressure (approximately

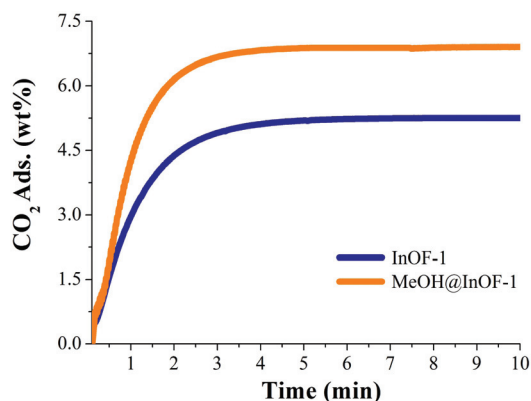


Fig. 4 Kinetic CO₂ uptake experiments performed at 303 K with a CO₂ flow of 60 mL min⁻¹ in InOF-1 (blue curve) and MeOH@InOF-1 (orange curve).

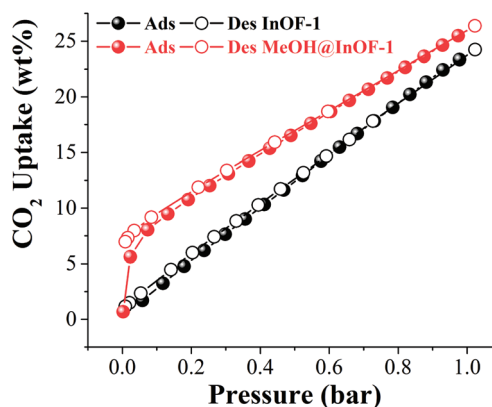


Fig. 5 Static CO₂ adsorption-desorption performed from 0 to 1 bar at 196 K on InOF-1 (black circles) and MeOH@InOF-1 (red circles).

Table 1 Adsorption properties of InOF-1 loaded with different solvents

Sample	BET surface area (m ² g ⁻¹)	pore volume (cm ³ g ⁻¹)	Solvent loading (wt%)	CO ₂ uptake (wt%)	
				Kinetic ^a (303 K)	Static ^b (196 K)
InOF-1	1066	0.37	0.00	5.24	1.14
MeOH@InOF-1	720	0.34	2	6.9	5.59
DMF@InOF-1 ¹⁶	628	0.32	4.2	8.06	7.14
EtOH@InOF-1 ^{17a}	514	0.28	2.6	14.14	—

^a CO₂ uptake at 1 bar and 60 mL min⁻¹ flux. ^b CO₂ uptake at 0.026 bar.

0.026 bar) of 5.59 wt%, (Fig. 5, MeOH@InOF-1). Conversely, the CO₂ uptake of InOF-1 at the same pressure was equal to 1.14 wt%. This result is interesting since at very low pressure, the CO₂ uptake is considerably enhanced (4.88-fold increase) by confining small amounts of MeOH. The total CO₂ uptake of MeOH@InOF-1 at 1 bar was 26.0 wt%, which in comparison with the InOF-1 sample, corresponds only to a small improvement (1.07-fold increase) (see Fig. 5). Both BET area (720 m² g⁻¹) and pore volume (0.34 cm³ g⁻¹) obtained for MeOH@InOF-1 are lower than the values for the empty InOF-1 (1065 m² g⁻¹ and 0.37 cm³ g⁻¹ respectively). These observations are consistent with other confined solvents (EtOH and DMF) @InOF-1 (see Table 1).¹⁶

Molecular simulations were further performed to gain insight into the adsorption behaviors of MeOH and CO₂ at the molecular level. The MC calculations evidenced that the μ₂-OH groups are the most preferential adsorption sites for both guests as mentioned above. However, since the adsorption enthalpy for MeOH (−40.8 kJ mol⁻¹) is significantly higher than for CO₂ (−21 kJ mol⁻¹) as single components, MeOH is favorably adsorbed around the μ₂-OH groups in a binary mixture and this geometry tends to screen the CO₂/μ₂-OH interactions as can be observed from Fig. 6.

Fig. S8† shows that the presence of MeOH leads to a small enhancement of the strength of CO₂/InOF-1 interactions from −21 kJ mol⁻¹ to −23 kJ mol⁻¹. The comparison between the van der Waals surface area plotted for the DFT-optimized empty InOF-1 and MeOH@InOF-1 structures demonstrates

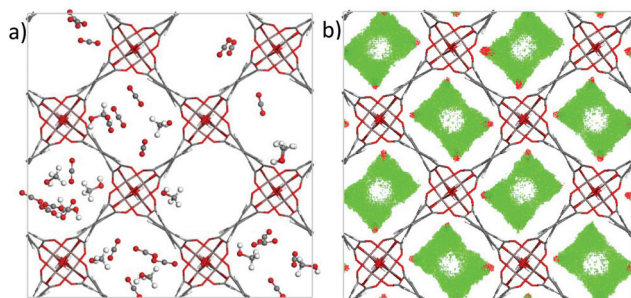


Fig. 6 Illustration of the preferential adsorption sites simulated by MC for both guests as a binary mixture in InOF-1 (a) and the map of the center of mass distribution of CO₂ (green region)/MeOH (red region) as a binary mixture averaged over all the configurations generated by MC simulations (b).

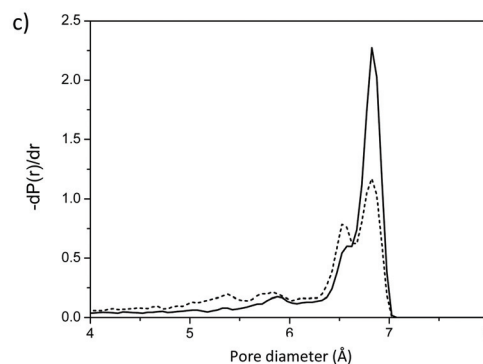
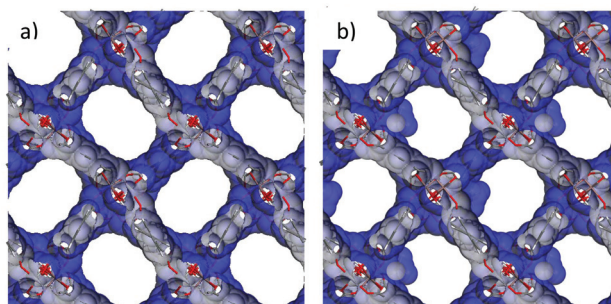


Fig. 7 van der Waals surface area plotted for the DFT-optimized empty InOF-1 (a) and MeOH@InOF-1 (b) structures. Comparison of the pore size distribution calculated for the two structures (empty InOF-1 solid lines and MeOH@InOF-1 dashed lines) (c).

that the presence of MeOH induces a decrease of the accessible porosity for CO₂, consistent with the experimental findings, by forming a lump at the vicinity of the μ₂-OH groups (Fig. 7b). This is also reflected in the plot of the pore size distribution for the two InOF-1 (Fig. 7c). This observation supports that the slightly higher CO₂ affinity of MeOH@InOF-1 as compared to the empty InOF-1 and hence the higher uptake is most probably caused by the higher degree of confinement felt by the adsorbed CO₂ in the presence of MeOH rather than a mutual energetic effect between the two guests.

Conclusions

The MeOH adsorption properties of InOF-1, a microporous In(III)-based MOF material, were first investigated. Rapid MeOH

uptakes and hysteresis loops at low loadings ($\%P/P_0 = 0$ to 10) at 303 and 293 K demonstrated a high affinity towards MeOH. This MeOH affinity was experimentally quantified by the evaluation of the isosteric heat of adsorption ($\Delta H = -41 \text{ kJ mol}^{-1}$) and confirmed by force field-based MC simulations ($\Delta H = -40.8 \text{ kJ mol}^{-1}$) while DFT geometry optimizations evidenced the formation of a relatively strong hydrogen bond between O(MeOH) and H(μ_2 -OH).

Kinetic isotherm CO_2 experiments showed a CO_2 uptake of 5.2 wt% for fully activated InOF-1. After confining small amounts of MeOH (2 wt%) within its micropores, the CO_2 capture, for MeOH@InOF-1, increased to 6.9 wt% corresponding to a 1.3-fold improvement. Static and isothermal CO_2 experiments (~ 0.026 bar and 196 K) exhibited a remarkable 4.88-fold CO_2 capture increase (from 1.14 wt%, for fully activated InOF-1 to 5.59 wt%, for MeOH@InOF-1).

MC calculations showed that MeOH forms a lump at the vicinity of the μ_2 -OH groups that tends to increase the degree of confinement felt by CO_2 , most probably at the origin of the higher CO_2 uptake observed in the low domain of pressure for MeOH@InOF-1 as compared to the empty solid.

Conflicts of interest

There are no conflicts to declare.

Acknowledgements

The authors thank Dr A. Tejeda-Cruz (X-ray; IIM-UNAM), PAPIIT UNAM (IN101517) and CONACyT (1789) Mexico for financial support. E. G.-Z. thanks CONACyT (236879), Mexico for financial support. Thanks to U. Winnberg (ITAM) for scientific discussions. P. G. M. Mileo thanks the National Counsel of Technological and Scientific Development (CONPQ) for the scholarship. G. M. thanks the Institut Universitaire de France for its support.

Notes and references

- 1 S. Miachon, V. V. Syakaev, A. Rakhmatullin, M. Pera-Titus, S. Caldarelli and J.-A. Dalmon, *ChemPhysChem*, 2008, **9**, 78.
- 2 (a) S. Clauzier, L. N. Ho, M. Pera-Titus, D. Farrusseng and B. Coasne, *J. Phys. Chem. C*, 2014, **118**, 10720; (b) L. N. Ho, Y. Schuurman, D. Farrusseng and B. Coasne, *J. Phys. Chem. C*, 2015, **119**, 21547.
- 3 (a) F. Volino, H. Gérard and S. Miachon, *Ann. Phys.*, 1997, **22**, 43; (b) K. Morishige and M. Shikimi, *J. Chem. Phys.*, 1998, **108**, 7821; (c) M. O. Kimball and F. M. Gasparini, *Phys. Rev. Lett.*, 2005, **95**, 165701; (d) U. Zammit, M. Marinelli, F. Mercuri and S. Paoloni, *J. Phys. Chem. B*, 2009, **113**, 14315.
- 4 X. Jiang, H.-B. Duan, S. I. Khan and M. A. Garcia-Garibay, *ACS Cent. Sci.*, 2016, **2**, 608.
- 5 (a) A. Luzar and D. Bratko, *J. Phys. Chem. B*, 2005, **109**, 22545; (b) D. Bratko and A. Luzar, *Langmuir*, 2008, **24**, 1247.
- 6 (a) M. Pera-Titus, R. El-Chahal, V. Rakotovao, S. Miachon and J.-A. Dalmon, *ChemPhysChem*, 2009, **10**, 2082; (b) M. Pera-Titus, S. Miachon and J.-A. Dalmon, *AIChE J.*, 2009, **55**, 434; (c) V. Rakotovao, R. Ammar, S. Miachon and M. Pera-Titus, *Chem. Phys. Lett.*, 2010, **485**, 299.
- 7 (a) N. L. Ho, J. Perez-Pellitero, F. Porcheron and R. J.-M. Pellenq, *J. Phys. Chem. C*, 2012, **116**, 3600; (b) N. L. Ho, J. Perez-Pellitero, F. Porcheron and R. J.-M. Pellenq, *Langmuir*, 2011, **27**, 8187; (c) N. L. Ho, F. Porcheron and R. J.-M. Pellenq, *Langmuir*, 2010, **26**, 13287.
- 8 S. Clauzier, L. N. Ho, M. Pera-Titus, B. Coasne and D. Farrusseng, *J. Am. Chem. Soc.*, 2012, **134**, 17369.
- 9 E. Soubeyrand-Lenoir, C. Vagner, J. W. Yoon, P. Bazin, F. Ragon, Y. K. Hwang, C. Serre, J.-S. Chang and P. L. Llewellyn, *J. Am. Chem. Soc.*, 2012, **134**, 10174.
- 10 R. A. Peralta, B. Alcántar-Vázquez, M. Sánchez-Serratos, E. González-Zamora and I. A. Ibarra, *Inorg. Chem. Front.*, 2015, **2**, 898.
- 11 J. R. Álvarez, R. A. Peralta, J. Balmaseda, E. González-Zamora and I. A. Ibarra, *Inorg. Chem. Front.*, 2015, **2**, 1080.
- 12 E. Sánchez-González, J. R. Álvarez, R. A. Peralta, A. Campos-Reales-Pineda, A. Tejeda-Cruz, E. Lima, J. Balmaseda, E. González-Zamora and I. A. Ibarra, *ACS Omega*, 2016, **1**, 305.
- 13 E. González-Zamora and I. A. Ibarra, *Mater. Chem. Front.*, 2017, **1**, 1471.
- 14 (a) H. Jasuja, Y.-G. Huang and K. S. Walton, *Langmuir*, 2012, **28**, 16874; (b) H. Jasuja, J. Zang, D. S. Sholl and K. S. Walton, *J. Phys. Chem. C*, 2012, **116**, 23526; (c) J. B. DeCoste, G. W. Peterson, H. Jasuja, T. G. Glover, Y.-G. Huang and K. S. Walton, *J. Mater. Chem. A*, 2013, **1**, 5642; (d) N. C. Burtch, H. Jasuja and K. S. Walton, *Chem. Rev.*, 2014, **114**, 10575; (e) G. E. Cmarik, M. Kim, S. M. Cohen and K. S. Walton, *Langmuir*, 2012, **28**, 15606.
- 15 (a) M. R. Gonzalez, J. H. González-Estefan, H. A. Lara-García, P. Sánchez-Camacho, E. I. Basaldella, H. Pfeiffer and I. A. Ibarra, *New J. Chem.*, 2015, **39**, 2400; (b) H. A. Lara-García, M. R. Gonzalez, J. H. González-Estefan, P. Sánchez-Camacho, E. Lima and I. A. Ibarra, *Inorg. Chem. Front.*, 2015, **2**, 442; (c) M. Sánchez-Serratos, P. A. Bayliss, R. A. Peralta, E. González-Zamora, E. Lima and I. A. Ibarra, *New J. Chem.*, 2016, **40**, 68; (d) A. Zárate, R. A. Peralta, P. A. Bayliss, R. Howie, M. Sánchez-Serratos, P. Carmona-Monroy, D. Solis-Ibarra, E. González-Zamora and I. A. Ibarra, *RSC Adv.*, 2016, **6**, 9978.
- 16 E. Sánchez-González, E. González-Zamora, D. Martínez-Otero, V. Jancik and I. A. Ibarra, *Inorg. Chem.*, 2017, **56**, 5863.
- 17 (a) R. A. Peralta, A. Campos-Reales-Pineda, H. Pfeiffer, J. R. Álvarez, J. A. Zárate, J. Balmaseda, E. González-Zamora, A. Martínez, D. Martínez-Otero, V. Jancik and I. A. Ibarra, *Chem. Commun.*, 2016, **52**, 10273; (b) J. R. Álvarez, E. Sánchez-González, E. Pérez,

- E. Schneider-Revueltas, A. Martínez, A. Tejada-Cruz, A. Islas-Jácome, E. González-Zamora and I. A. Ibarra, *Dalton Trans.*, 2017, **46**, 9192.
- 18 G. A. González-Martínez, J. A. Zárate, A. Martínez, E. Sánchez-González, J. R. Álvarez, E. Lima, E. González-Zamora and I. A. Ibarra, *RSC Adv.*, 2017, **7**, 24833.
- 19 (a) D. M. D'Alessandro, B. Smit and J. R. Long, *Angew. Chem., Int. Ed.*, 2010, **49**, 6058; (b) K. Sumida, D. L. Rogow, J. A. Mason, T. M. McDonald, E. D. Bloch, Z. R. Herm, Z. T.-H. Bae and J. R. Long, *Chem. Rev.*, 2012, **112**, 724.
- 20 (a) S. Yang, G. S. B. Martin, J. J. Titman, A. J. Blake, D. R. Allan, N. R. Champness and M. Schröder, *Inorg. Chem.*, 2011, **50**, 9374; (b) S. Yang, X. Lin, A. J. Blake, G. S. Walker, P. Hubberstey, N. R. Champness and M. Schröder, *Nat. Chem.*, 2009, **1**, 487; (c) A. J. Nuñez, L. N. Shear, N. Dahal, I. A. Ibarra, J. W. Yoon, Y. K. Hwang, J.-S. Chang and S. M. Humphrey, *Chem. Commun.*, 2011, **47**, 11855; (d) I. A. Ibarra, J. W. Yoon, J.-S. Chang, S. K. Lee, V. M. Lynch and S. M. Humphrey, *Inorg. Chem.*, 2012, **51**, 12242; (e) X. Lin, A. J. Blake, C. Wilson, X. Z. Sun, N. R. Champness, M. W. George, P. Hubberstey, R. Mokaya and M. Schröder, *J. Am. Chem. Soc.*, 2006, **128**, 10745; (f) P. Nugent, Y. Belmabkhout, S. D. Burd, A. J. Cairns, R. Luebke, K. Forrest, T. Pham, S. Ma, B. Space, L. Wojtas, M. Eddaoudi and M. J. Zaworotko, *Nature*, 2013, **495**, 80; (g) O. Shekhah, Y. Belmabkhout, Z. Chen, V. Guillermin, A. Cairns, K. Adil and M. Eddaoudi, *Nat. Commun.*, 2014, **5**, 522; (h) W. M. Bloch, A. Burgun, C. J. Coghlan, R. Lee, M. L. Coote, C. J. Doonan and C. J. Sumby, *Nat. Chem.*, 2014, **6**, 906; (i) K. Okada, R. Ricco, Y. Tokudome, M. J. Styles, A. J. Hill, M. Takahashi and P. Falcaro, *Adv. Funct. Mater.*, 2014, **24**, 1969; (j) H. Li, M. R. Hill, R. Huang, C. Doblin, S. Lim, A. J. Hill, R. Babarao and P. Falcaro, *Chem. Commun.*, 2016, **52**, 5973; (k) K. Sumida, N. Moitra, J. Reboul, S. Fukumoto, K. Nakanishi, K. Kanamori, S. Furukawa and S. Kitagawa, *Chem. Sci.*, 2015, **6**, 5938; (l) K. Hirai, S. Furukawa, M. Kondo, H. Uehara, O. Sakata and S. Kitagawa, *Angew. Chem., Int. Ed.*, 2011, **50**, 8057.
- 21 (a) T. Tozawa, J. T. A. Jones, S. I. Swamy, S. Jiang, D. J. Adams, S. Shakespeare, R. Clowes, D. Bradshaw, T. Hasell, S. Y. Chong, C. Tang, S. Thompson, J. Parker, A. Trewin, J. Bacsá, A. M. Z. Slawin, A. Steiner and A. I. Cooper, *Nat. Mater.*, 2009, **8**, 973; (b) R. Dawson, D. J. Adams and A. I. Cooper, *Chem. Sci.*, 2011, **2**, 1173; (c) W. M. Bloch, R. Babarao, M. R. Hill, C. J. Doonan and C. J. Sumby, *J. Am. Chem. Soc.*, 2013, **135**, 10441; (d) J. A. Mason, K. Sumida, Z. R. Herm, R. Krishna and J. R. Long, *Energy Environ. Sci.*, 2011, **4**, 3030; (e) R. Babarao, C. J. Coghlan, D. Rankine, W. M. Bloch, G. K. Gransbury, H. Sato, S. Kitagawa, C. J. Sumby, M. R. Hill and C. J. Doonan, *Chem. Commun.*, 2014, **50**, 3238; (f) I. A. Ibarra, A. Mace, S. Yang, J. Sun, S. Lee, J.-S. Chang, A. Laaksonen, M. Schröder and X. Zou, *Inorg. Chem.*, 2016, **55**, 7219; (g) A. López-Olvera, E. Sánchez-González, A. Campos-Reales-Pineda, A. Aguilar-Granda, I. A. Ibarra and B. Rodríguez-Molina, *Inorg. Chem. Front.*, 2017, **4**, 56.
- 22 M. Poliakoff, W. Leitner and E. S. Streng, *Faraday Discuss.*, 2015, **183**, 9.
- 23 J. Qian, F. Jiang, D. Yuan, M. Wu, S. Zhang, L. Zhang and M. Hong, *Chem. Commun.*, 2012, **48**, 9696.
- 24 I. A. Ibarra, S. Yang, X. Lin, A. J. Blake, P. J. Rizkallan, H. Nowell, D. R. Allan, N. R. Champness, P. Hubberstey and M. Schröder, *Chem. Commun.*, 2011, **47**, 8304.
- 25 (a) J. P. Perdew, K. Burke and M. Ernzerhof, *Phys. Rev. Lett.*, 1996, **77**, 3865; (b) J. P. Perdew, K. Burke and M. Ernzerhof, *Phys. Rev. Lett.*, 1997, **78**, 1396.
- 26 (a) B. Delley, *J. Chem. Phys.*, 1990, **92**, 508; (b) B. Delley, *J. Chem. Phys.*, 2000, **113**, 7756.
- 27 J. G. Harris and K. H. Yung, *J. Phys. Chem.*, 1995, **99**, 12021.
- 28 D. F. Plant, G. Maurin and R. Bell, *J. Phys. Chem. B*, 2007, **111**, 2836.
- 29 A. K. K. Rappé, C. J. J. Casewit, K. S. S. Colwell, W. A. Goddard III and W. M. Skiff, *J. Am. Chem. Soc.*, 1992, **114**, 10024.
- 30 S. L. Mayo, B. D. Olafson and W. A. Goddard III, *J. Phys. Chem.*, 1990, **101**, 8897.
- 31 (a) I. A. Ibarra, X. Lin, S. Yang, A. J. Blake, G. S. Walker, S. A. Barnett, D. R. Allan, N. R. Champness, P. Hubberstey and M. Schröder, *Chem. – Eur. J.*, 2010, **16**, 13671; (b) I. A. Ibarra, T. W. Hesterberg, B. J. Holliday, V. M. Lynch and S. M. Humphrey, *Dalton Trans.*, 2012, **41**, 8003; (c) I. A. Ibarra, P. A. Bayliss, E. Pérez, S. Yang, A. J. Blake, H. Nowell, D. R. Allan, M. Poliakoff and M. Schröder, *Green Chem.*, 2012, **14**, 117; (d) A. M. Bohnsack, I. A. Ibarra, V. I. Bakhmutov, V. M. Lynch and S. M. Humphrey, *J. Am. Chem. Soc.*, 2013, **135**, 16038; (e) A. J. Nuñez, M. S. Chang, I. A. Ibarra and S. M. Humphrey, *Inorg. Chem.*, 2014, **53**, 282.
- 32 D. R. Lide, *Handbook of Chemistry and Physics*, CRC Press LLC, 84th edn, 2004.
- 33 M. F. de Lange, K. J. F. M. Verouden, T. J. H. Vlugt, J. Gascon and F. Kapteijn, *Chem. Rev.*, 2015, **115**, 12205.
- 34 (a) X. B. Zhao, B. Xiao, A. J. Fletcher, K. M. Thomas, D. Bradshaw and M. J. Rosseinsky, *Science*, 2004, **306**, 1012; (b) H. J. Choi, M. Dincă and J. R. Long, *J. Am. Chem. Soc.*, 2008, **130**, 7848; (c) O. M. Linder-Patton, W. M. Bloch, C. J. Coghlan, K. Sumida, S. Kitagawa, S. Furukawa, C. J. Doonan and C. J. Sumby, *CrystEngComm*, 2016, **18**, 4172.
- 35 G. R. Medders and F. Paesani, *J. Phys. Chem. Lett.*, 2014, **5**, 2897.
- 36 V. Haigis, F.-X. Coudert, R. Vuilleumier and A. Boutin, *Phys. Chem. Chem. Phys.*, 2013, **15**, 19049.
- 37 F. Salles, S. Bourrelly, H. Jobic, T. Devic, V. Guillermin, P. Llewellyn, C. Serre, G. Férey and G. Maurin, *J. Phys. Chem. C*, 2011, **115**, 10764.
- 38 F. Rouquerol, J. Rouquerol, K. S. W. Sing, P. Llewellyn and G. Maurin, *Adsorption by Powders and Porous Solids; Principles, Methodology and Applications*, Elsevier Press, 2014.

- 39 J. Garrido, A. Linares-Solano, J. M. Martín-Martínez, M. Molina-Sabio, F. Rodríguez-Reinoso and R. Torregrosa, *Langmuir*, 1987, **3**, 76.
- 40 (a) H. J. Park and M. P. Sun, *Chem. – Eur. J.*, 2008, **14**, 8812; (b) S. M. Humphrey, J.-S. Chang, S. H. Jhung, J. W. Yoon and P. T. Wood, *Angew. Chem., Int. Ed.*, 2007, **46**, 272; (c) J. Lee, N. W. Waggoner, L. Polanco, G. R. You, V. M. Lynch, S. K. Kim, S. M. Humphrey and J. L. Sessler, *Chem. Commun.*, 2016, **52**, 8514; (d) A. Aguilar-Granda, S. Pérez-Estrada, E. Sánchez-González, J. R. Álvarez, J. Rodríguez-Hernández, M. Rodríguez, A. E. Roa, S. Hernández-Ortega, I. A. Ibarra and B. Rodríguez-Molina, *J. Am. Chem. Soc.*, 2017, **139**, 7549.